A Necessary Model to Quantify the Scanning Loss Effect in Spaceborne iGNSS-R Ocean Altimetry

Zongqiang Liu, Wei Zheng, Fan Wu, Zhen Cui, and Guohua Kang

***Abstract*—When the interferometric global navigation satellite system reflectometry (iGNSS-R) altimeter receives the direct and reflected signals through the digital multibeam phased array antenna, the roll-off of element radiation pattern will cause the scanning loss of directivity. If the scanning loss is neglected, the ocean altimetric precision will be biased with possible consequences for the instrument design. This article carries out the following research on this. First, based on the geometry of iGNSS-R altimetry and the principle of phased array antenna beamformer, the scanning loss model with the elevation angle at the specular point as a parameter is established. Second, this article uses the measured data of the phased array antenna to verify the model, and the result shows that the simulated value is in good agreement with the measured value, with an average deviation of 0.07 dB. Third, taking the GPS L1 signal (full composite) as an example, the model is used to analyze the influence of the scanning loss on the iGNSS-R altimetric precision estimation. The research results show that when the phased array antenna synthesizes four beams for iGNSS-R altimetry, the comprehensive effect of scanning loss on altimetric precision estimation is 0.16 m. The influence of scanning loss should be considered in the future high-precision iGNSS-R altimetry instrument design.**

***Index Terms*—Altimetric precision estimation, antenna directivity, digital multibeam phased array antenna, interferometric global navigation satellite system reflectometry (iGNSS-R), ocean altimetry, scanning loss model, TechDemoSat-1 (TDS-1).**

I. Introduction

THE global navigation satellite system reflectometry (GNSS-R) ocean altimetry is an innovative and powerful earth observation technology integrating satellite navigation and remote sensing, which can raise the possibility of measuring ocean mesoscale variability [1], [2]. Since the passive reflectometry and interferometric system (PARIS) was first proposed in 1993 [3], the feasibility of GNSS-R ocean altimetry has been verified on shore-based, airborne, and spaceborne platforms [4]–[11], and further improving the precision of altimetry is the key to promote its application. The sea surface height (SSH) with high precision can effectively improve the inversion accuracy of the physical ocean model, which is helpful to the study of ocean dynamics and global climate change.

The currently implemented spaceborne GNSS-R scattering missions all use the hereafter conventional GNSS-R (cGNSS-R) [12], such as U.K. disaster monitoring constellation (U.K.-DMC) [13], TechDemoSat-1 (TDS-1) [14], 3Cat-2 [15], cyclone global navigation satellite system (CYGNSS) [16], and BuFeng-1 (BF-1) A/B twin satellites [17]. The satellites as mentioned above are equipped with a single- or two-directional antennas to receive the reflected signals. We proposed the nadir antenna observation capability optimization method to increase the number of sea surface reflected signals received by cGNSS-R satellite [18]. However, these spaceborne GNSS-R missions are mainly used for wind speed retrieval rather than ocean altimetry. Among them, the error of using the TDS-1 and the CYGNSS observations to retrieve SSH is above 2.5 m (1 Hz) [7], [8], which is because the directional antennas with low directivity (less than 15 dB), resulting in low signal-to-noise ratio (SNR) of the received signal, and the bandwidth of the C/A code (2.046 MHz) is relatively narrow [19]. These two factors limit the performance of cGNSS-R ocean altimetry. In order to overcome the limitation of signal bandwidth, Martin-Neira *et al*. successively proposed the concept and model of interferometric GNSS (iGNSS-R) [3], [20]. Compared with the cGNSS-R altimetry, the iGNSS-R altimetry can extract all the spectral components in the GNSS signals and improve the altimetric precision by the sharper autocorrelation function [21]. Since the correlation between the direct signal and the reflected signal and the increase of signal bandwidth will bring higher thermal noise, it is necessary to use the direct and reflected signal receiving antenna with a higher directivity to improve the SNR. Besides, the iGNSS-R altimetry cannot distinguish GNSS satellites based on the code structure and requires the antenna to synthesize multiple beams with variable directions to simultaneously capture and track multiple GNSS direct and reflected signals (as shown in Fig. 1). Therefore, the digital multibeam phased array antenna with high directivity (greater than 20 dB) is the key instrument for the high precision of the spaceborne iGNSS-R ocean altimetry.

Manuscript received August 14, 2020; revised October 30, 2020, November 30, 2020, and December 16, 2020; accepted December 16, 2020. Date of publication December 23, 2020; date of current version January 11, 2021. This work was supported by the National Nature Science Foundation of China under Grant 41774014 and Grant 41574014, in part by the Frontier Science and Technology Innovation Project under Grant 085015, and in part by the Innovation Workstation Project of the Science and Technology Commission of the Central Military Commission, and the Outstanding Youth Foundation of the China Academy of Space Technology *(Zongqiang Liu, Wei Zheng, and Fan Wu contributed equally to this work). (Corresponding authors: Wei Zheng; Fan Wu.)*

Zongqiang Liu and Guohua Kang are with the School of Astronautics, Nanjing University of Aeronautics and Astronautics, Nanjing 210016, China (e-mail: bestlzq@nuaa.edu.cn; kanggh@nuaa.edu.cn).

Wei Zheng and Fan Wu are with the Qian Xuesen Laboratory of Space Technology, China Academy of Space Technology, Beijing 100094, China (e-mail: zhengwei1@qxslab.cn; wufan@qxslab.cn).

Zhen Cui is with the Xian Institute of Space Radio Technology, China Academy of Space Technology, Xian 710100, China (e-mail: cuizhen@stu.xidian.edu.cn).

Digital Object Identifier 10.1109/JSTARS.2020.3046729

This work is licensed under a Creative Commons Attribution 4.0 License. For more information, see https://creativecommons.org/licenses/by/4.0/

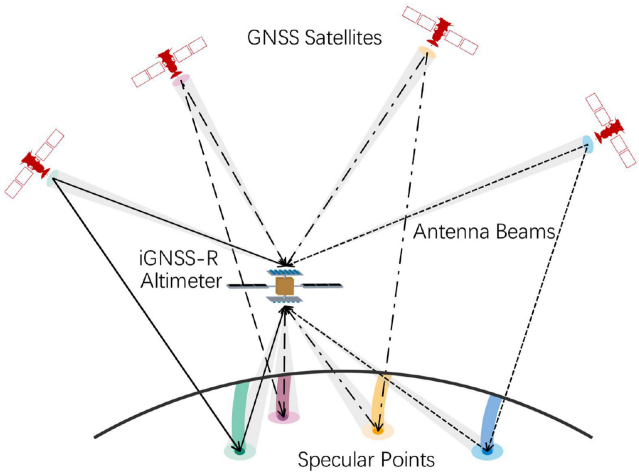

Fig. 1. Scheme of the iGNSS-R altimeter theoretical method.

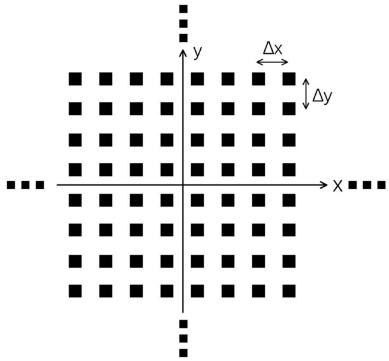

Fig. 2. 2-D digital multibeam phased array antenna.

Currently, no GNSS-R altimeter has been launched. However, the future spaceborne GNSS-R altimetry missions issued by European Space Agency (ESA) all use the analog multibeam phased array antennas, such as PARIS In-orbit Demonstrator (PARIS IoD) [20], GNSS reflectometry, radio occultation, and scatterometry onboard the International Space Station (GEROS-ISS) [22], "Cookie" satellite [23], and GNSS Transpolar Earth Reflectometry exploriNg system (G-TERN) [24]. Therefore, the evaluation of iGNSS-R altimetry performance based on antenna parameters is very important for the instrument design. When the up-looking and down-looking digital multibeam phased array antennas, respectively, receive the GNSS direct signals and the reflected signals, the gain peak of the scanning beam will be directed to the transmitter and the specular point (SP) through the power splitter and phase shifter. The digital multibeam phased array antenna parameters that affect the performance of iGNSS-R altimetry mainly include the directivity, the scanning angle (beam pointing), and the number of beams. The most typical feature of the digital multibeam phased array antenna is the ability to electronically scan the beam. However, in the process of beam scanning, the antenna pattern will be loss due to the downward trend of the array element pattern, which is the so-called "scanning loss." In other words, the directivity of the scanning beam decreases with the increase of the scanning angle, which can be up to 10 dB [25]. Therefore, if the directivity of the scanning beam is determined as a constant, it will bring deviation in the estimation of altimetry performance.

At present, relevant scholars have considered the scanning loss when studying the influence of the antenna directivity on the iGNSS-R altimetry performance. In 2014, Camps *et al*. proposed a method for optimizing the iGNSS-R altimeter configuration, and applied it to the PARIS IOD to estimate the SNR when the directivity is 15–25 dB, and the values of scanning loss are set to 2.8 and 1.6 dB [26]. In 2017, Camps *et al*. evaluated the GEROS-ISS ocean altimetry performance and proposed that the noise of the GEROS antenna beamformer (GAB) including scanning loss is not higher than 3.5 dB, and considered the sensitivity of the altimetry error to the antenna directivity. Then, this factor was considered and analyzed the sensitivity of the altimetry error to the antenna directivity [27]. However, there is no established scanning loss model for the scenario of spaceborne iGNSS-R ocean altimetry to analyze the influence of scanning loss on altimetry performance estimation.

Different from previous studies, in order to analyze the influence of scanning loss on altimetry performance estimation, this article establishes a scanning loss model for the scenario of spaceborne iGNSS-R ocean altimetry for the first time. The scanning loss of the up-looking and down-looking digital multibeam phased array antennas at different elevation angles can be obtained through this model. Then, taking TDS-1 as an example, the model is used to comprehensively evaluate the influence of scanning loss on altimetric precision estimation.

II. Construction and Verification of the Scanning Loss Model

A. Construction

The directivity is an important parameter that affects the estimation of iGNSS-R ocean altimetric precision. The new scanning loss model can more accurately estimate the up-looking and down-looking antenna's directivity at different positions, thereby more accurately estimating the iGNSS-R ocean altimetric precision.

The digital multibeam phased array antenna has the ability to scan the beam so that the beam has a maximum gain at the scan angle. By applying the appropriate phase at each element, the antenna beam can be moved spatially without physically moving the entire array. For phase steering, each element has a phase shifter and applies the appropriate phase as a function of frequency and scan angle. Taking the 2-D digital multibeam phased array antenna as an example (as shown in Fig. 2), the down-looking antenna's pattern expression for phase delay steering can be expressed as [25]

$$D_{\mathrm{R}}(\xi_{\mathrm{R}},\varphi_{\mathrm{R}}) = \mathrm{EP}(\xi_{\mathrm{R}}) \cdot \sum_{i=1}^{M\cdot N} c_i^{\mathrm{R}} e^{j\left(\frac{2\pi}{\lambda}x_i \sin\xi_{\mathrm{R}}\cos\varphi_{\mathrm{R}} + \frac{2\pi}{\lambda}y_i \sin\xi_{\mathrm{R}}\sin\varphi_{\mathrm{R}}\right)} \cdot e^{-j\left(\frac{2\pi}{\lambda}x_i \sin\xi_0^{\mathrm{R}}\cos\varphi_0^{\mathrm{R}} + \frac{2\pi}{\lambda}y_i \sin\xi_0^{\mathrm{R}}\sin\varphi_0^{\mathrm{R}}\right)} \quad (1)$$

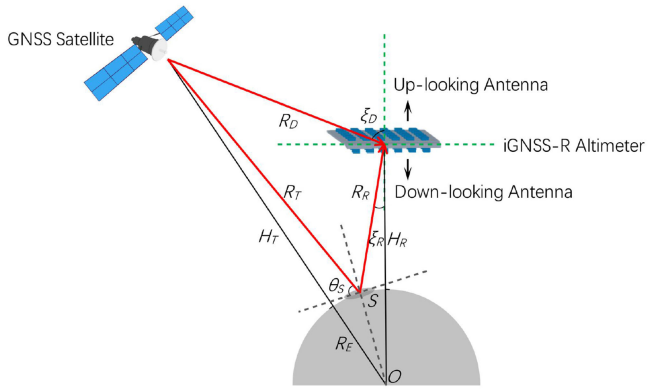

Fig. 3. Bistatic geometry involved in the iGNSS-R altimetry, where o is the geo-centre, s is the position of the SP, θ_s is the elevation angle, R_E is the earth radius, H_T and H_R are the orbital altitude of the GNSS satellite and the iGNSS-R altimeter, respectively, R_T is the reflected signal transmission distance from GNSS satellite to the SP, R_R is the reflected signal reception distance from the SP to the iGNSS-R altimeter, and R_D is the direct signal transmission distance from GNSS satellite to the iGNSS-R altimeter.

where ξ_{R} and φ_{R} are the complement to the elevation angle and azimuth angle of the receiver relative to the SP, respectively. The EP is the antenna element radiation pattern, which can be defined as $\cos^{\mathrm{EF}/2}\xi_{\mathrm{R}}$. The EF is the element factor, and its value depends on the radiator design. The M and N are the number of elements in the x-dimension and the y-dimension, c_i^{R} is the complex voltage at each element, ξ_0^{R} and φ_0^{R} are the scanning beam pointing, x_i and y_j are the x–y element positions in the array with $x_i = (i - 0.5(M+1)) \cdot \Delta x$ and $y_i = (j - 0.5(N+1)) \cdot \Delta y$, and Δx Δy are the element spacing in the x-dimension and the y-dimension.

The directivity at the boresight is usually used directly when estimating iGNSS-R altimetry performance. But in the operation of the digital multibeam phased array antenna, the directivity will change with the scanning angle.

Without considering the beam pointing error, the direction of the scanning beam will point to the SP. In other words, the complement to the elevation angle and azimuth angle of the receiver relative to the SP is consistent with the scanning beam pointing. Then, the directivity taper of the scanning beam (i.e., the scanning loss) can be expressed as a function related to the elevation angle of the scanning direction based on (1)

$$D_{\mathrm{R}}^{\mathrm{loss}}(\xi_{\mathrm{R}}) = \cos^{\mathrm{EF}/2}\xi_{\mathrm{R}} \cdot \sum_{i=1}^{M \cdot N} c_i^{\mathrm{R}}. \tag{2}$$

Similarly, the directivity of the scanning beam of the up-looking digital multibeam phased array antenna can also be expressed as

$$D_{\mathrm{D}}^{\mathrm{loss}}(\xi_{\mathrm{D}}) = \cos^{\mathrm{EF}/2}\xi_{\mathrm{D}} \cdot \sum_{i=1}^{M \cdot N} c_i^{\mathrm{D}} \tag{3}$$

where ξ_{D} is the complement to the elevation angle of the up-looking antenna relative to the GNSS satellite.

According to the bistatic geometry of iGNSS-R (as shown in Fig. 3), ξ_{R} and ξ_{D} can be expressed by the satellite elevation angle at the SP

$$\xi_{\mathrm{R}} = \arcsin\left(\frac{R_{\mathrm{E}}\cos\theta_{\mathrm{S}}}{H_{\mathrm{R}} + R_{\mathrm{E}}}\right) \tag{4}$$

$$\xi_{\mathrm{D}} = \pi - \xi_{\mathrm{R}} - \arcsin\left(\frac{R_{\mathrm{T}}\sin 2\theta_{\mathrm{S}}}{R_{\mathrm{D}}}\right). \tag{5}$$

The signal transmission distance can be obtained by triangular geometry

$$\begin{cases} R_{\mathrm{T}} = -R_{\mathrm{E}} \cdot \sin\theta_{\mathrm{S}} + \sqrt{(H_{\mathrm{T}} + R_{\mathrm{E}})^2 - R_{\mathrm{E}}^2 \cdot \cos^2\theta_{\mathrm{S}}} \\ R_{\mathrm{R}} = -R_{\mathrm{E}} \cdot \sin\theta_{\mathrm{S}} + \sqrt{(H_{\mathrm{R}} + R_{\mathrm{E}})^2 - R_{\mathrm{E}}^2 \cdot \cos^2\theta_{\mathrm{S}}} \\ R_{\mathrm{D}} = \sqrt{R_{\mathrm{T}}^2 + R_{\mathrm{R}}^2 + 2R_{\mathrm{T}} \cdot R_{\mathrm{R}} \cdot \cos 2\theta_{\mathrm{S}}} \end{cases}. \tag{6}$$

The scanning loss of the up-looking and down-looking antennas at the SP can be expressed as a function of θ_{S}

$$D_{\mathrm{D}}^{\mathrm{loss}}(\theta_{\mathrm{S}}) = -\cos^{\mathrm{EF}/2}\left[\arcsin\left(\frac{R_{\mathrm{E}}\cos\theta_{\mathrm{S}}}{H_{\mathrm{R}} + R_{\mathrm{E}}}\right) + \arcsin\left(\frac{R_{\mathrm{T}}\sin\theta_{\mathrm{S}}}{R_{\mathrm{D}}}\right)\right] \cdot \sum_{i=1}^{M \cdot N} c_i^{\mathrm{D}} \tag{7}$$

$$D_{\mathrm{R}}^{\mathrm{loss}}(\theta_S) = \cos^{\mathrm{EF}/2}\left[\arcsin\left(\frac{R_{\mathrm{E}}\cos\theta_{\mathrm{S}}}{H_{\mathrm{R}} + R_{\mathrm{E}}}\right)\right] \cdot \sum_{i=1}^{M \cdot N} c_i^{\mathrm{R}}. \tag{8}$$

Equations (7) and (8) are the scanning loss models of the iGNSS-R altimeter up-looking and down-looking digital multibeam phased array antenna. The new scanning loss model is the theoretical basis of this study, and the research results obtained by this model provide a data basis for the iGNSS-R altimetry performance analysis in Section III.

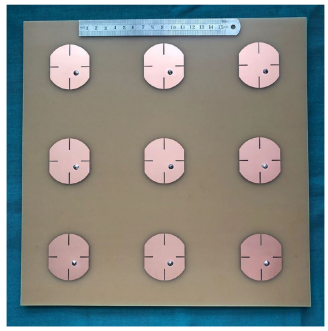

Fig. 4. Prototype of the proposed antenna array.

B. Verification

After the optimization and fabrication, an exclusive antenna array is designed and manufactured (as shown in Fig. 4). The antenna array is connected with the beam-forming network, and the scanning loss is tested by the WILTRON37269A network analyzer in an anechoic chamber. The beams scanning at the range of 0–45 degree was measured respectively in order to get the scanning loss of the antenna. The measured data are used to verify the new scanning loss model. The specific parameters of the antenna are shown in Table I.

TABLE I
PARAMETERS OF THE PROPOSED ANTENNA

Parameter	Value
Antenna Aperture (mm×mm)	300×300
Elements Number (unit)	9（3×3）
Center Frequency (MHz)	1575.42
Frequency Bandwidth (MHz)	10
Polarization	LHCP
Axis Ratio (dB)	<3
Beam Width (°)	41.3
Directivity at the boresight (dB)	14.1

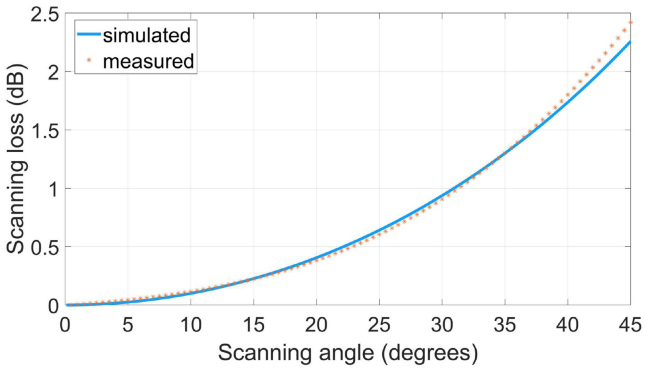

Fig. 5. Difference between the simulated data based on the model and the measured data.

According to (2) and the parameters in Table I, the simulated results are obtained (as shown in Fig. 5). The EF is set to 1.5 [25]. It can be seen from Fig. 5 that the measured data and the simulated data are in good agreement. The scanning loss model proposed in this article is based on (2) and obtained through geometric relationship conversion, so it can be proved that the model can express the actual scanning loss well. The average deviation between the measured data and the simulated data is 0.07 dB, which is due to signal coupling between adjacent elements. The energy of one element in the array will enter the adjacent element and then stimulate the adjacent element's secondary radiation. The signal of the secondary radiation is superimposed with the current signal to form the pattern of the phased array antenna, and this superposition must comprehensively consider the amplitude and phase characteristics of each element.

III. RESULTS AND DISCUSSIONS

The scanning loss leads to a deviation in the estimation of the cross-correlated signal power and directly affects the SNR estimation. Meanwhile, the SNR is a key factor affecting iGNSS-R ocean altimetric precision. Therefore, the scanning loss finally leads to the deviation of the estimation of iGNSS-R ocean altimetric precision. This section obtains the scanning loss at different elevation angles according to the scanning loss model, and then analyzes the influence of the scanning loss on the SNR and precision estimation of the iGNSS-R ocean altimetry.

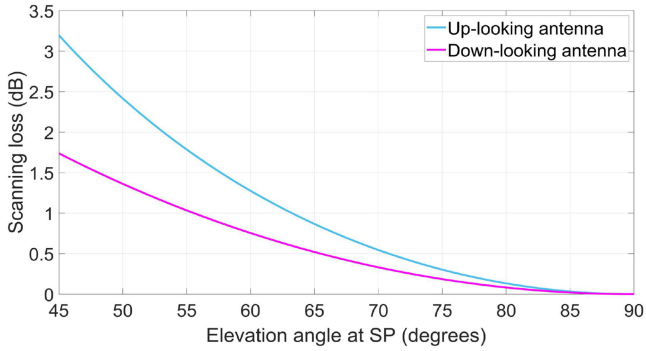

Fig. 6. Scanning loss as a function of elevation angle at SP.

A. Scanning Loss

It can be seen from (7) and (8) that when the digital multibeam phased array antenna is applied to iGNSS-R altimetry, the main factors affecting the scanning loss are the altimeter orbit altitude and the elevation angle at the SP. In the present study, taking the TDS-1 orbit altitude (635 km) as an example, the scanning loss at the elevation angle of 45°–90° was calculated (as shown in Fig. 6).

It can be seen from Fig. 6 that the scanning loss gradually decreases as the elevation angle increases. Compared with the down-looking antenna, the up-looking antenna's scanning loss is more obvious, which is determined by the iGNSS-R altimetry geometry. The scanning loss of the two antennas differs by up to 1.5 dB.

B. Signal to Thermal Noise Ratio

The scanning loss has a direct impact on iGNSS-R SNR estimation. The iGNSS-R altimetry obtains the delay through the cross correlation of the reflected signal and the direct signal. Therefore, the thermal noise of the up-looking channel and the average cross-correlated noise need to be additionally considered when calculating the SNR. The iGNSS-R SNR at correlator's output is given by [20]

$$\begin{aligned}\mathrm{SNR_{iR}}(\tau) &= \frac{\left\langle |Y_{\mathrm{S}}(\tau)|^2 \right\rangle}{\left\langle |Y_{\mathrm{N}}(\tau)|^2 \right\rangle} \\ &= \frac{\left\langle |Y_{\mathrm{S}}(\tau)|^2 \right\rangle}{\left\langle |Y_{\mathrm{Nd}}(\tau)|^2 \right\rangle + \left\langle |Y_{\mathrm{Nr}}(\tau)|^2 \right\rangle + \left\langle |Y_{\mathrm{Ndr}}(\tau)|^2 \right\rangle} \\ &= \frac{\mathrm{SNR_{cr}}(\tau)\,\mathrm{SNR_{D,in}}(\tau)}{1+\mathrm{SNR_{R,in}}(\tau)+\mathrm{SNR_{D,in}}(\tau)} \end{aligned} \tag{9}$$

where $\langle |Y_{\mathrm{S}}(\tau)|^2 \rangle$ and $\langle |Y_{\mathrm{N}}(\tau)|^2 \rangle$ are signal power and thermal noise power, respectively, $\langle |Y_{\mathrm{Nd}}(\tau)|^2 \rangle$ and $\langle |Y_{\mathrm{Nr}}(\tau)|^2 \rangle$ are the thermal noise power of the up-looking channel and the down-looking channel, respectively, and $\langle |Y_{\mathrm{Ndr}}(\tau)|^2 \rangle$ is the cross-correlation power of the up-looking noise and the down-looking noise. The $\mathrm{SNR_{cr}}(\tau)$, $\mathrm{SNR_{D,in}}(\tau)$, and $\mathrm{SNR_{R,in}}(\tau)$ are the

TABLE II
PARAMETERS OF THE PROPOSED ANTENNA

Parameter	Value	
GNSS-R satellite orbital altitude (km)	635	
Elevation angle at SP (°)	55 / 75	
Receiver bandwidth (MHz)	40	
Signal bandwidth (MHz)	40 (GPS L1 Full Composite)	
Signal frequency (MHz)	1575.42	
EIRP (dBw)	34 (optimistic)	
Antenna equivalent noise temperature (K)	up-looking	500
	down-looking	550
Antenna radiation efficiency (%)	100	
Wind speed at sea level (m/s)	10	
Coherent integration time (ms)	1	

*EIRP: Equivalent isotropically radiated power.

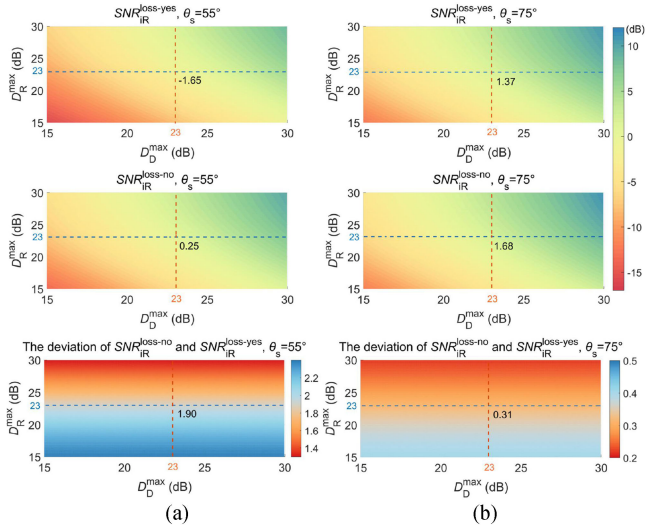

Fig. 7. iGNSS-R SNR and deviation as a function of directivity at the boresight considering or not the scanning loss. (a) Elevation angle is 55°. (b) Elevation angle is 75°.

SNRs of the clean-replica cross-correlation, direct, and reflected signal, respectively [28].

In this study, the scenario of the TDS-1 was used to evaluate the iGNSS-R altimetry performance, so the system parameters of the iGNSS-R altimeter were as consistent as possible with TDS-1 (as shown in Table II).

Unlike cGNSS-R altimetry which only uses L1 C/A code, this study uses GPS L1 full composite (C/A code, P code, M code, and inter-modulation components) [21], [29]. Combining the parameters given in Table II and (7), (8), and (9), the SNR when scanning loss is considered ($\mathrm{SNR}_{\mathrm{iR}}^{\mathrm{loss-yes}}$), the SNR when scanning loss is neglected ($\mathrm{SNR}_{\mathrm{iR}}^{\mathrm{loss-no}}$), and the deviation $\Delta\mathrm{SNR}_{\mathrm{iR}} = \mathrm{SNR}_{\mathrm{iR}}^{\mathrm{loss-no}} - \mathrm{SNR}_{\mathrm{iR}}^{\mathrm{loss-yes}}$ is calculated separately. The results are shown in Fig. 7 and Table III.

It can be seen from Fig. 7 and Table III that as the directivity at the boresight of the up-looking and down-looking antennas increases, the influence of the scanning loss on the estimation of the SNR can be reduced. Furthermore, the influence of the scanning loss on the estimation of the SNR is more obvious in the region with a lower elevation angle. This is because as the elevation angle decreases, the up-looking and down-looking antennas' scanning angles become larger, resulting in the more significant loss of the scanning beam's directivity.

TABLE III
IGNSS-R SNR UNDER DIFFERENT DIRECTIVITY AT THE BORESIGHT

Elevation angle (°)	SNR (dB)	Up-looking and down-looking antenna's directivity at the boresight (dB)			
		15	20	25	30
55	$SNR_{\mathrm{iR}}^{\mathrm{loss-yes}}$	-16.02	-6.72	1.61	8.51
	$SNR_{\mathrm{iR}}^{\mathrm{loss-no}}$	-13.64	-4.59	3.32	9.81
	ΔSNR_{iR}	2.38	1.87	1.71	1.30
75	$SNR_{\mathrm{iR}}^{\mathrm{loss-yes}}$	-12.46	-3.44	4.42	10.87
	$SNR_{\mathrm{iR}}^{\mathrm{loss-no}}$	-12.05	-3.08	4.70	11.09
	ΔSNR_{iR}	0.41	0.36	0.28	0.22

C. Altimetric Precision

The estimation of iGNSS-R altimetric precision is crucial for the reasonable design and size determination of the digital multibeam phased array antenna. Since the SNR is the main factor determining the precision of the iGNSS-R altimetry, the scanning loss will also affect the precision estimation. The scanning loss impact analysis on the precision estimation is based on the precision model provided in [20]

$$\sigma_{\mathrm{iR}}\left(D_{\mathrm{D}}^{\mathrm{loss}}, D_{\mathrm{R}}^{\mathrm{loss}}\right) = \frac{\sqrt{\left(1+\frac{1}{\mathrm{SNR}_{\mathrm{iR}}\left(D_{\mathrm{D}}^{\mathrm{loss}}, D_{\mathrm{R}}^{\mathrm{loss}}\right)}\right)^2 + \left(\frac{1}{\mathrm{SNR}_{\mathrm{iR}}\left(D_{\mathrm{D}}^{\mathrm{loss}}, D_{\mathrm{R}}^{\mathrm{loss}}\right)}\right)^2}}{2\sin\theta_{\mathrm{S}} \cdot \psi_{\mathrm{SSH}}\sqrt{N_{\mathrm{incoh}}}} \tag{10}$$

where N_{incoh} is the number of samples incoherently averaged, ψ_{SSH} is the altimetric sensitivity, which can be considered to depend on the autocorrelation properties of the transmitted signal in a spaceborne scenario with $\psi_{\mathrm{SSH}} = \bar{P}'_{\mathrm{R,S}}/c\bar{P}_{\mathrm{R,S}}$, $\bar{P}_{\mathrm{R,S}}$, and $\bar{P}'_{\mathrm{R,S}}$ are the averaged power amplitude at the SP and the leading derivative of the power waveform respectively [30], and c is the speed of light in vacuum.

1) Precision Estimation Under Different Directivity at the Boresight: According to the relevant parameters in Table II, (10), and the SNR results obtained in Section III-B, the altimetric precision when scanning loss is considered ($\sigma_{\mathrm{iR}}^{\mathrm{loss-yes}}$), the altimetric precision when scanning loss is neglected ($\sigma_{\mathrm{iR}}^{\mathrm{loss-no}}$), and the deviation $\Delta\sigma_{\mathrm{iR}} = \sigma_{\mathrm{iR}}^{\mathrm{loss-yes}} - \sigma_{\mathrm{iR}}^{\mathrm{loss-no}}$ is calculated separately. The number of incoherent averages is set to 1000 and the results are shown in Fig. 8 and Table IV.

It can be seen from Fig. 8 and Table IV that by increasing the directivity at the boresight of the up-looking and down-looking

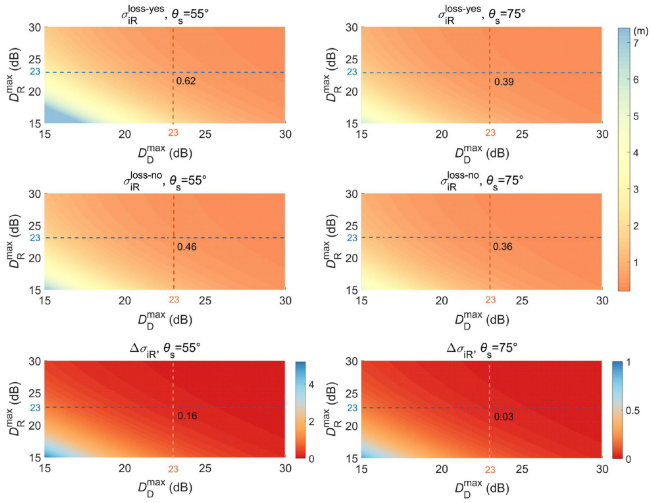

Fig. 8. iGNSS-R altimetric precision and deviation as a function of the directivity at the boresight considering or not the scanning loss. (a) Elevation angle is 55°. (b) Elevation angle is 75°.

TABLE IV
iGNSS-R ALTIMETRIC PRECISION UNDER DIFFERENT DIRECTIVITY AT THE BORESIGHT

Elevation angle (°)	Altimetric precision (m)	Up-looking and down-looking antennas directivity at the boresight (dB)			
		15	20	25	30
55	$\sigma_{iR}^{loss\text{-}yes}$	12.40	1.60	0.40	0.25
	$\sigma_{iR}^{loss\text{-}no}$	7.23	1.04	0.33	0.24
	$\Delta\sigma_{iR}$	5.17	0.56	0.07	0.01
75	$\sigma_{iR}^{loss\text{-}yes}$	5.97	0.87	0.28	0.21
	$\sigma_{iR}^{loss\text{-}no}$	5.07	0.77	0.27	0.20
	$\Delta\sigma_{iR}$	0.90	0.10	0.01	0.01

antennas, the altimetric precision can be significantly improved, which shows the dependence of the altimetric precision on the SNR. The improvement of the directivity at the boresight can also reduce the influence of scanning loss on altimetric precision. Also, the influence of scanning loss on altimetric precision varies significantly at different elevation angles. Compared with the altitude angle of 75°, the effect increases by the order of magnitude when the altitude angle is 55°. This shows that the greater the elevation angle, the smaller the impact of scanning loss on precision estimation. More GNSS satellites can provide better geometric configurations for iGNSS-R altimetry. Therefore, the iGNSS-R receiver should be designed for future fully operational global multi-GNSS.

2) Comprehensive Evaluation: Take TDS-1 as an Example: From the analysis in Section III-C1, it can be seen that when the elevation angle is high (greater than 75°), the scanning loss has little effect on the altimetric precision estimation. However,

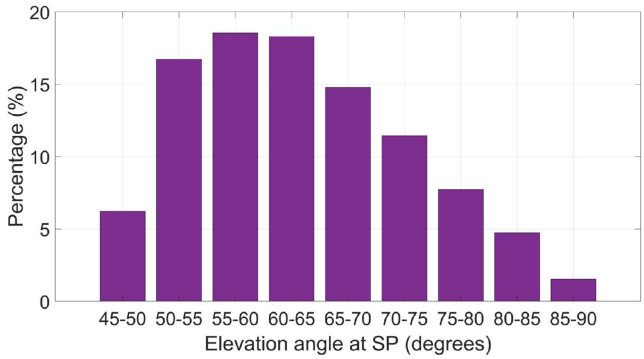

Fig. 9. Elevation angle statistics of the TDS-1 SPs within 24 h.

relatively few reflection events occurred in this range during observation. This article comprehensively evaluates the influence of the scanning loss on the altimetric precision estimation using the observations of the TDS-1.

The Surrey Satellite Technology Limited used the quasispherical Earth approach to calculate the position and elevation angle of the TDS-1 SPs (1 Hz) and published in the L1b products [14]. The data of 169482 SPs with 24 h from March 1, 2018 20:00:00 h to March 2, 2018 20:00:00 h were used in the present study. Fig. 9 shows the elevation angle statistics of the SPs. It can be seen from Fig. 9 that 86.01% of the reflection events within 24 hours occurred in the range of 45°–75°.

Based on the elevation angle, the altimetric precision of the TDS-1 SPs is calculated according to the parameters in Table II and (10) (as shown in Fig. 10). Among them, the directivity at the boresight of the up-looking and down-looking antennas is set to 23 dB. The precision statistics curve on the right-hand side of Fig. 10 is obtained after averaging every 100 precision results. It should be noted that since the iGNSS-R needs to use the direct signal, the scanning angle of the up-looking antenna (θ_D) should be higher than 0°. Under this restriction, when the orbital altitude of the receiver and transmitter is 635 and 20 200 km, the minimum elevation angle at the SP is 15.31°. The minimum elevation angle in the TDS-1 observations is 45.51°, so the SPs shown in Fig. 10 meet this requirement.

It can be seen from Fig. 10 that there is a deviation in altimetric precision between considering and not considering the scanning loss, which is more evident in the polar areas. This is due to the inadequate geometric coverage of the GNSS satellites in this area, resulting in a low elevation angle for receiving reflected signals. The TDS-1 observations only recorded GPS signals. It is expected that with more GNSS signal sources, the precision deviation caused by the scanning loss will be reduced.

Fig. 11 shows the altimetric precision estimation results corresponding to the elevation angle. It can be seen from Fig. 11 that in the area with an elevation angle of 45°–65°, the deviation of precision estimation caused by the scanning loss reaches more than 5 cm, and it can be seen from Fig. 9 that the distribution of the SPs in this area is dense. In order to comprehensively evaluate the influence of the scanning loss on the altimetric precision estimation, the elevation angle range (45°–90°) is divided into

TABLE V
STATISTICS OF THE ALTIMETRIC PRECISION DEVIATION AND THE SPS DISTRIBUTION

Elevation angle (degrees)	45~50	50~55	55~60	60~65	65~70	70~75	75~80	80~85	85~90
$\Delta\bar{\sigma}_{\mathrm{iR}}$ (m)	0.75	0.34	0.17	0.08	0.04	0.02	7.91e-03	2.79e-03	5.40e-04
p (%)	6.23	16.73	18.54	18.29	14.77	11.44	7.72	4.73	1.54

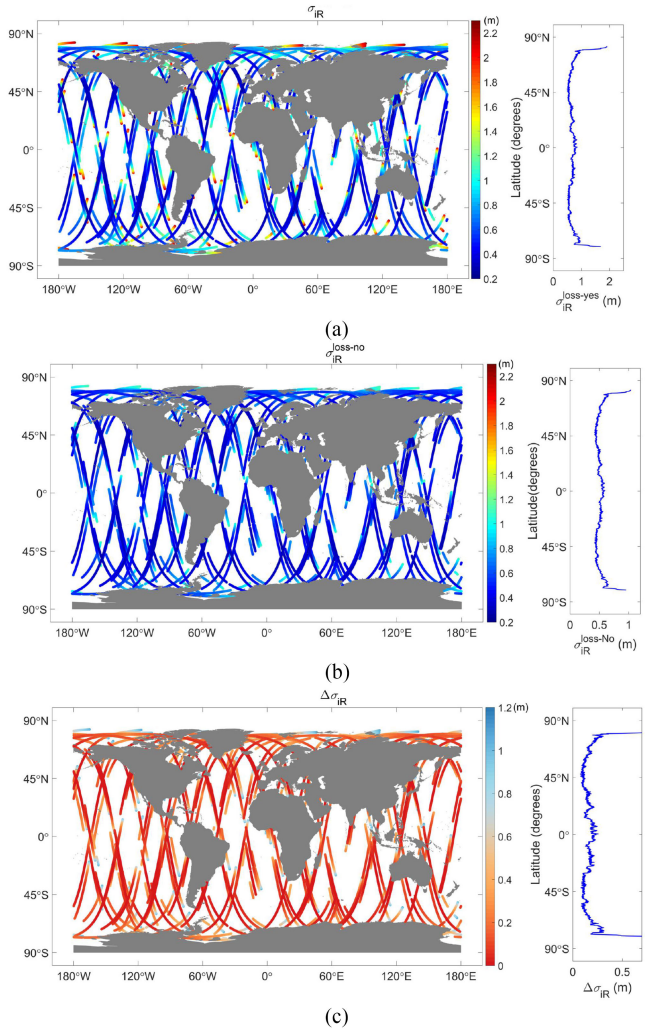

Fig. 10. iGNSS-R altimetric precision and deviation corresponding to the position of the SPs with 24 h. (a) Altimetric precision considering the scanning loss ($\sigma_{\mathrm{iR}}^{\mathrm{loss-yes}}$). (b) Altimetric precision neglecting the scanning loss ($\sigma_{\mathrm{iR}}^{\mathrm{loss-no}}$). (c) Altimetric precision deviation $\Delta\sigma_{\mathrm{iR}} = \sigma_{\mathrm{iR}}^{\mathrm{loss-yes}} - \sigma_{\mathrm{iR}}^{\mathrm{loss-no}}$.

nine parts, and the average altimetric precision deviation of each part ($\Delta\bar{\sigma}_{\mathrm{iR}}$) and the proportion ($p$) of the SPs are counted (as shown in Table V).

Then perform a weighted average of the results in Table V, i.e., $\Delta\sigma^{\mathrm{cpx}} = \sum_{q=1}^{k} \Delta\bar{\sigma}_{\mathrm{iR}}(q)p_q$, where $\Delta\sigma^{\mathrm{cpx}}$ is the altimetric precision comprehensive deviation and q is the elevation angle intervals. The results show that the comprehensive effect

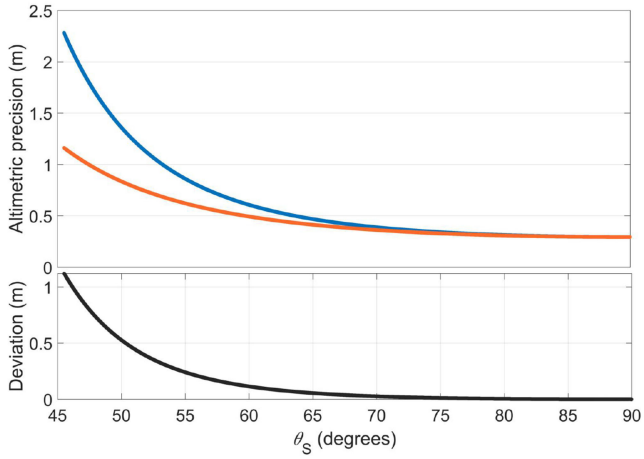

Fig. 11. iGNSS-R altimetric precision and deviation as a function of the elevation angle at SP.

of scanning loss on altimetric precision estimation is 0.16 m. Therefore, the design of future spaceborne iGNSS-R altimetry missions needs to consider changes in antenna directivity caused by the beam scanning.

IV. CONCLUSION

This work has established a scanning loss model suitable for the spaceborne iGNSS-R altimetry scenario based on the iGNSS-R geometry and the principle of digital multibeam phased array antenna. The model is verified by the measured data of a 3 × 3 phased array antenna. Applying the scanning loss model, taking GPS L1 signal (full composite) as an example, the influence of the scanning loss on altimetry performance estimation is systematically analyzed. According to the research results, the following conclusions are obtained. First, compared with the down-looking antenna, the up-looking antenna's scanning loss is more prominent, which is determined by the iGNSS-R altimetric geometry. Second, the influence of scanning loss on the altimetric SNR and precision estimation is more evident in areas with low elevation angles, and this influence can be reduced by increasing the antenna directivity at the boresight. Third, combined with of TDS-124 h observations, the comprehensive analysis found that the scanning loss caused a deviation of 0.16 m in the altimetric precision estimation. It is worth noting that the TDS-1 only uses GPS satellites as the illuminator, and its satellite geometry is not as good as that of

multi-GNSS systems. If the future iGNSS-R altimetry mission will be designed for future fully operational global multi-GNSS, the influence of the scanning loss on altimetry performance estimation will be reduced.

The scanning loss model proposed in this article can effectively quantify the effect of scanning loss on the iGNSS-R altimetry performance estimation, which provides a theoretical basis for the design of future high-precision spaceborne iGNSS-R altimetry missions.

ACKNOWLEDGMENT

The authors would like to thank Surrey Satellite Technology Limited (SSTL) for providing GNSS-R data acquired from the TDS-1 mission that have been used in this study.

REFERENCES

[1] Z. Li, C. Zuffada, S. T. Lowe, T. Lee, and V. Zlotnicki, "Analysis of GNSS-R altimetry for mapping ocean mesoscale sea surface heights using high-resolution model simulations," *IEEE J. Sel. Topics Appl. Earth Observ.*, vol. 9, no. 10, pp. 4631–4642, Oct. 2016.

[2] J. Saynisch, M. Semmling, J. Wickert, and M. J. O. D. Thomas, "Potential of space-borne GNSS reflectometry to constrain simulations of the ocean circulation," *Ocean Dyn.*, vol. 65, no. 11, pp. 1441–1460, Sep. 2015.

[3] M. Martin-Neira, "A passive reflectometry and interferometry system (PARIS): Application to ocean altimetry," *ESA J.*, vol. 17, no. 4, pp. 331–355, Dec. 1993.

[4] M. Martín-Neira, M. Caparrini, J. Font-Rossello, S. Lannelongue, and C. S. Vallmitjana, "The PARIS concept: An experimental demonstration of sea surface altimetry using GPS reflected signals," *IEEE Trans. Geosci. Remote Sens.*, vol. 39, no. 1, pp. 142–149, Jan. 2001.

[5] G. Ruffini, F. Soulat, M. Caparrini, O. Germain, and M. Martin-Neira, "The Eddy experiment: Accurate GNSS-R ocean altimetry from low altitude aircraft," *Geophys. Res. Lett.*, vol. 31, no. 12, Jun. 2004, Art. no. L12306.

[6] A. Rius, E. Cardellach, and M. Martin-Neira, "Altimetric analysis of the sea-surface GPS-Reflected signals," *IEEE Trans. Geosci. Remote Sens.*, vol. 48, no. 4, pp. 2119–2127, Apr. 2010.

[7] M. P. Clarizia, C. Ruf, P. Cipollini, and C. J. G. R. L. Zuffada, "First spaceborne observation of sea surface height using GPS-Reflectometry," *Geophys. Res. Lett.*, vol. 43, no. 2, pp. 767–774, Jan. 2016.

[8] W. Li, E. Cardellach, F. Fabra, S. Ribó, and A. Rius, "Assessment of spaceborne GNSS-R ocean altimetry performance using CYGNSS mission raw data," *IEEE Trans. Geosci. Remote Sens.*, vol. 58, no. 1, pp. 238–250, Aug. 2019.

[9] E. Cardellach *et al.*, "First precise spaceborne sea surface altimetry with GNSS reflected signals," *IEEE J. Sel. Topics Appl. Earth Observ. Remote Sens.*, vol. 13, pp. 102–112, Dec. 2019.

[10] F. Fabra *et al.*, "Phase altimetry with dual polarization GNSS-R over sea ice," *IEEE Trans. Geosci. Remote Sens.*, vol. 50, no. 99, pp. 2112–2121, Jun. 2012.

[11] W. Li, E. Cardellach, F. Fabra, A. Rius, S. Ribó, and M. Martín-Neira, "First spaceborne phase altimetry over sea ice using Techdemosat-1 GNSS-R signals," *Geophys. Res. Lett.*, vol. 44, no. 16, pp. 8369–8376, Aug. 2017.

[12] V. Zavorotny, S. Gleason, E. Cardellach, A. J. I. G. Camps, and R. S. Magazine, "Tutorial on remote sensing using GNSS bistatic radar of opportunity," *IEEE Geosci. Remote Sens. Lett.*, vol. 2, no. 4, pp. 8–45, Jan. 2015.

[13] M. J. Unwin, S. Gleason, and M. Brennan, "The space GPS reflectometry experiment on the U.K. disaster monitoring constellation satellite," in *Proc. ION-GPS/GNSS*, Portland, OR, USA, Sep. 2003.

[14] Jales, P. and M. Unwin, "MERRByS product manual: GNSS-Reflectometry on TDS-1 with the SGR-ReSI," Surrey Satellite Technol. Ltd., Guilford, England, Tech. Rep. SSTL Rep. 0248366 Revision 001, 2017. [Online]. Available: http://www.merrbys.co.uk

[15] H. Carreno-Luengo *et al.*, "3Cat-2—An Experimental nanosatellite for GNSS-R earth observation: Mission concept and analysis," *IEEE J. Sel. Topics Appl. Earth Observ. Remote Sens.*, vol. 9, no. 10, pp. 4540–4551, May 2016.

[16] C. S. Ruf *et al.*, "New ocean winds satellite mission to probe hurricanes and tropical convection," *Bull. Amer. Meteorol. Soc.*, vol. 97, no. 3, pp. 385–395, Mar. 2016.

[17] C. Jing, X. Niu, C. Duan, F. Lu, G. Di, and X. Yang, "Sea surface wind speed retrieval from the first Chinese GNSS-R mission: Technique and preliminary results," *Remote Sens.*, vol. 11, no. 24, Dec. 2019, Art. no. 3013.

[18] Z. Liu *et al.*, "Increasing the number of sea surface reflected signals received by GNSS-reflectometry altimetry satellite using the nadir antenna observation capability optimization method," *Remote Sens.*, vol. 11, no. 21, Oct. 2019, Art. no. 2473.

[19] F. Martin, A. Camps, H. Park, S. Daaddio, M. Martin-Neira, and D. Pascual, "Cross-correlation waveform analysis for conventional and interferometric GNSS-R approaches," *IEEE J. Sel. Topics Appl. Earth Observ. Remote Sens.*, vol. 7, no. 5, pp. 1560–1572, Jun. 2014.

[20] M. Martin-Neira, S. D'Addio, C. Buck, N. Floury, and R. Prieto-Cerdeira, "The PARIS ocean altimeter in-orbit demonstrator," *IEEE Trans. Geosci. Remote Sens.*, vol. 49, no. 6, pp. 2209–2237, Jun. 2011.

[21] W. Li *et al.*, "The impact of inter-modulation components on interferometric GNSS-reflectometry," *Remote Sens.*, vol. 8, no. 12, Dec. 2016, Art. no. 1013.

[22] J. Wickert *et al.*, "GEROS-ISS: GNSS reflectometry, radio occultation, and scatterometry onboard the international space station," *IEEE J. Sel. Topics Appl. Earth Observ. Remote Sens.*, vol. 9, no. 10, pp. 4552–4581, Oct. 2016.

[23] M. Martín-Neira, W. Li, A. Andrés-Beivide, and X. Ballesteros-Sels, ""Cookie": A satellite concept for GNSS remote sensing constellations," *IEEE J. Sel. Topics Appl. Earth Observ. Remote Sens.*, vol. 9, no. 10, pp. 4593–4610, Jun. 2016.

[24] E. Cardellach *et al.*, "GNSS transpolar earth reflectometry exploring system (G-TERN): Mission concept," *IEEE Access*, vol. 6, pp. 13980–14018, Mar. 2018.

[25] A. D. Brown, *Electronically Scanned Arrays: MATLAB Modeling and Simulation*. Boca Raton, FL, USA: CRC-Press, 2012, pp. 36–63.

[26] A. Camps *et al.*, "Optimization and performance analysis of interferometric GNSS-R altimeters: Application to the PARIS IoD mission," *IEEE J. Sel. Topics Appl. Earth Observ. Remote Sens.*, vol. 7, no. 5, pp. 1436–1451, May 2014.

[27] A. Camps, H. Park, I. Sekulic, and J. M. Rius, "GNSS-R altimetry performance analysis for the GEROS experiment on board the international space station," *Sensors*, vol. 17, no. 7, Jul. 2017, Art. no. 1583.

[28] V. Zavorotny and A. G. Voronovich, "Scattering of GPS signals from the ocean with wind remote sensing application," *IEEE Trans. Geosci. Remote Sens.*, vol. 38, no. 2, pp. 951–964, Mar. 2000.

[29] D. Pascual, H. Park, A. Camps, A. A. Arroyo, and R. Onrubia, "Simulation and analysis of GNSS-R composite waveforms using GPS and Galileo signals," *IEEE J. Sel. Topics Appl. Earth Observ. Remote Sens.*, vol. 7, no. 5, pp. 1461–1468, May 2014.

[30] W. Li, A. Rius, F. Fabra, E. Cardellach, S. Ribó, and M. Martín-Neira, "Revisiting the GNSS-R waveform statistics and its impact on altimetric retrievals," *IEEE Trans. Geosci. Remote Sens.*, vol. 56, no. 5, pp. 2854–2871, Dec. 2017.

Zongqiang Liu received the M.Sc. degree in geomatics from the Shandong University of Science and Technology, Qingdao, China, in 2018. He is currently working toward the Ph.D. degree in control science and engineering at the College of Astronautics, Nanjing University of Aeronautics and Astronautics, Nanjing, China.

He has also participated in the joint Ph.D. program in Qian Xuesen Laboratory of Technology, China Academy of Space Technology, Beijing, China. His research interests include the study of the global navigation satellite system reflectometry (GNSS-R) ocean altimetry, including the design of spaceborne antenna, and the reflection signal processing methods.

Wei Zheng received the Ph.D. degree from the Huazhong University of Science and Technology, Wuhan, China, and Postdoctoral degree from Kyoto University, Kyoto, Japan.

He worked with the Institute of Geodesy and Geophysics, Chinese Academy of Sciences, Beijing, China, and currently he is a Professor with the Qian Xuesen Laboratory of Space Technology, China Academy of Space Technology. He has published more than 80 research papers as the first author (39 papers included in SCI), and has published more than 40 research papers included in SCI as the corresponding author and coauthor. In addition, he has published four academic monographs in Science Press as an independent/first author. His research interests include satellite gravity recovery and the navigation and detection based on the information of aerospace—aeronautics–marine integration.

Fan Wu received the Ph.D. degree in ocean detection technology from the Ocean University of China, Qingdao, China, in 2017.

He participated in joint Ph.D. program supported by China Scholarship Council in the University of Rhode Island, Kingston, RI, USA, from 2014 to 2016. Since 2017, he has been with Qian Xuesen Laboratory of Technology, CAST, Beijing, China. He is currently the Co-Investigator of GNSS-R altimetry test satelllite mission. His research interests include GNSS-R sea surface altimetry and satellite ocean remote sensing on sea surface temperature and sea ice.

Zhen Cui received the B.Sc. and M.Sc. degrees from Xidian University, Xian, China, in 2006 and 2009, respectively.

He is currently working as an Engineer with the Xian Institute of Space Radio Technology, Xian, China. His key responsibilities include design, optimization, and capacity analysis for spaceborne antenna. He is also actively involved in China Academy of Space Technology (CAST) programs. His research interests include spaceborne antennas, global navigation satellite system reflectometry (GNSS-R) payload systems, and spaceborne remote sensing.

Guohua Kang received the Ph.D. degree from the Nanjing University of Aeronautics and Astronautics, Nanjing, China, in 2006.

He is a Researcher with the Nanjing University of Aeronautics and Astronautics. His research interests include microsatellite attitude and orbit control, navigation technology of the Beidou/GPS, multisensor information fusion, and satellite positioning and integrated navigation.